Progress In Electromagnetics Research M, Vol. 109, 231–240, 2022

Deep Learning Based Non-Iterative Solution to the Inverse Problem in Microwave Imaging

Ria Benny*, Thathamkulam A. Anjit, and Palayyan Mythili

Abstract—A deep learning-based approach in conjugation with Fourier Diffraction Theorem (FDT) is proposed in this paper to solve the inverse scattering problem arising in microwave imaging. The proposed methodology is adept in generating a permittivity mapping of the object in less than a second and hence has the potential for real-time imaging. The reconstruction of the dielectric permittivity from the measured scattered field values is done in a single step as against that by a long iterative procedure employed by conventional numerical methods. The proposed technique proceeds in two stages; with the initial estimate of the contrast function being generated by the FDT in the first stage. This initial profile is fed to a trained U-net to reconstruct the final dielectric permittivities of the scatterer in the second stage. The capability of the proposed method is compared with other works in the recent literature using the Root Mean Square Error (RMSE). The proposed method generates an RMSE of 0.0672 in comparison to similar deep learning methods like Back Propagation-Direct Sampling Method (BP-DSM) and Subspace-Based Variational Born Iterative Method (SVBIM), which produce error values 0.1070 and 0.0813 in the case of simulation (using Austria Profile). The RMSE level while reconstructing the experimental data (FoamDielExt experimental database) is 0.0922 for the proposed method as against 0.1631 and 0.1037 for BP-DSM and SVBIM, respectively.

1. INTRODUCTION

Microwave Imaging (MWI) is a noninvasive and non-ionizing imaging technology with an immense potential to cater to various industrial and bio-medical applications like nondestructive testing and evaluation, through-the-wall imaging, geological explorations, ageing and structural health monitoring, surveillance and remote sensing, medical imaging, etc. [1, 2]. While qualitative MWI can only retrieve the shape and location of the scatterers within the imaging domain, systems based on quantitative MWI aim to obtain a complete permittivity profile of the scatterer from the knowledge of measured scattered-field data arising from the illumination of the object under study by microwave energy. Recovering parameters that describe the physical state of a system (permittivity in this case) from measurements require the solving of an inverse problem [3]. Unlike the forward problem which is direct and linear, the electromagnetic Inverse Scattering Problem (ISP) is ill-posed in nature. Ill-posedness means that either non-existence or non-uniqueness of solution occurs during the inversion process, or otherwise, the determined solutions may suffer from instability issues [4]. The non-linearity and thereby, ill-posedness arises due to effects of multiple scattering [5].

The solution to the ISP can be easily formulated by decomposing the nonlinear equation into several linear equations using non-iterative techniques such as Born or Rytov approximation and back propagation. Such non-iterative methods do produce reconstruction results with shorter execution times, but are not effective for handling high contrast scenarios involving strong scatterers [5].

Received 9 January 2022, Accepted 29 March 2022, Scheduled 10 April 2022
* Corresponding author: Ria Benny (riabenny2802@gmail.com).
The authors are with the Cochin University of Science and Technology, Cochin, Kerala, India.

The conventional iterative inversion methods are either deterministic or stochastic in nature. They proceed by minimizing the objective function that quantifies the mismatch between calculated and measured data iteratively. Deterministic techniques like Born Iterative Method (BIM), Distorted Born Iterative Method (DBIM), Contrast Source Inversion, etc. deal with the minimization of a deterministic function. However, they have a tendency to get trapped at local minima. Stochastic methods (e.g., genetic algorithm and simulated annealing) on the other hand converge at the global optimum by following a probabilistic modeling. This is however achieved at the cost of a high computational burden. Due to the highly ill-posed nature of the ISP, inversion algorithms are in general combined with regularization schemes to arrive at the required quantitative solution. The main drawback of these regularized iterative methods is that they are time consuming and hence not suitable for real-time imaging [5].

With the advent of Compressive Sensing (CS), inverse problems started to be increasingly solved by researchers in the sparse domain. The key idea of compressive sensing is to recover a sparse signal from a very few nonadaptive linear measurements by convex optimization. Methods based on l_1 and l_0 minimization like Iterative Shrinkage Thresholding Algorithms (ISTA), Subspace pursuit, Orthogonal matching Pursuit, etc. were commonly employed to simplify the inversion process. However, these CS methods have many practical difficulties to handle. The scattered data from which inversion must be done is not inherently sparse in nature [6]. Further, enforcing Restricted Isometric Property (RIP) condition upon the scattered data, which is obtained by performing experiments, is not a feasible option. Additionally, the computational burden imposed by this class of methods and the slow rate of convergence limits the CS to non-real-time applications [3].

Motivated by the rapid development of computing hardware capable of handling large amount of data, Deep Learning (DL) techniques have already made significant contributions in the fields of image segmentation, super resolution, image denoising, regression, etc. [3]. It has been observed in the recent past that DL approaches have the potential to be a key problem-solver in the field of computational electromagnetics as well. Researchers in the MWI field make use of the Convolutional Neural Network (CNN) to solve the electromagnetic inverse scattering problem, which employs learnable weights and biases. The prime benefit in employing artificial intelligence in MWI is that real-time quantitative imaging is made possible due to its single-step implementation. The testing process can be completed in a few seconds as compared to several minutes and even hours in the case of complex inversion algorithms. One of the earliest works reported in this field was by Jin et al. [7] in which back-propagation algorithm was used to generate the seed images (initial contrast function) for training the DL network. In the two-step method, Yao et al. have employed two consecutive complex-valued CNNs, one network to generate the initial contrast function and the next to produce the refined final output image [6]. The Subspace-Based Variational Born Iterative Method (SVBIM) [2] in combination with U-net is reported to produce higher resolution images than the ordinary Born Iteration Method (BIM). Such recent works clearly demonstrate the efficiency and feasibility of employing DL in solving the inverse scatering problem in MWI.

In this paper, Fourier Diffraction Theorem (FDT) approach is combined with a U-net based DL network to solve the complex ISP encountered in quantitative MWI. Two types of entirely different databases (MNIST and dataset of circles) are used to train the network to be capable of reconstructing the permittivity profile of objects of varied shapes and sizes. The method proposed in this work is capable of generating better-resolution-images of the object under study (simulation and experimental) in comparison to the other works reported in this field. The reason for the enhanced results can be attributed to the finer initial contrast profile generated by the application of Fourier diffraction theorem. Experimental validation is also performed using the 'FoamDielExt' data provided by Fresnel Institute, thereby, proving the efficiency of the proposed method. Further, the improved performance of the proposed method has been validated by comparing it with the results reported by Zhang et al. (2020) [8] and Anjit et al. (2021) [2]. This paper is organized as follows. Section 2 describes the linear approximation of the ISP using Fourier diffraction theorem, and further, the DL network-based approach used to solve the inverse problem has been elaborated. The permittivity profile reconstruction results produced by the method proposed in this paper are described in Section 3. Finally, Section 4 concludes the paper.

2. PROBLEM STATEMENT

This paper proposes a two-dimensional (2D) non-iterative quantitative approach for solving the ill-posed ISP. The block diagram shown in Figure 1 depicts the methodology adopted to retrieve the dielectric profile of the scatterer. The object under study is illuminated using Transverse Magnetic (TM) waves, and these incident waves are scattered around in all directions due to the inhomogeneity introduced by the object. The Fourier diffraction theorem is adopted to produce the initial contrast function from the scattered signals received at the antennas. This initial estimate of the permittivity profile is given as input to the the deep learning module for the training process. In the testing phase, the U-net-based trained DL network produces the final refined output which is the permittivity profile of the object under test.

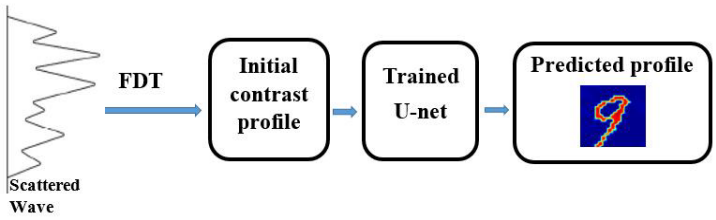

Figure 1. Block diagram of the proposed methodology for solving the ISP.

2.1. Fourier Diffraction Theorem in Inverse Scattering

Diffraction is related to spreading of waves upon interaction with an object in the medium. Diffraction tomography belongs to the class of inverse problems which is referred to be an improperly posed problem in the sense that a small variation in the measured value causes a large variation in the reconstructed model. By applying the principles of FDT, a one-step solving method for handling the complex inverse problems observed in quantitative microwave tomographic imaging is made possible.

In MWI, plane waves (defined by $E_{inc}(r) = e^{-jk_b\theta_0 r}$) are allowed to impinge the object under study (scatterer). The waves that reach the object are scattered around in all directions and collected by receiver antennas. The total electric field in the imaging domain is the superposition of the incident plane wave field, $E_{inc}(r)$ (without the object) and the scattered waves, $E_{scat}(r)$ (caused by the object) which are bouncing back from the inhomogeneity.

$$E_{tot}(r) = E_{inc}(r) + E_{scat}(r) \tag{1}$$

The Electric Field Integral Equation (EFIE) gives the complete expression for the total field at any point in the imaging domain. Suppose that $G_b(r, r')$ is the Green's function, k_0 the wave-number of the background medium, and $k(r)$ a scalar function denoting the wavenumber of the inhomogeneous region that in turn represents the contrast profile of the object, $c(r)$. If r is any point in the object domain-V, then the total field, $E_{tot}(r)$, is given by the EFIE as:

$$E_{tot}(r) = E_{inc}(r) + \int_V G_b(r, r')[k^2(r') - k_0^2(r')]E_{tot}(r')dr' \tag{2}$$

The above equation is nonlinear in nature because the unknown $E_{tot}(r)$ appears on both sides of the integral equation thereby making it ill-posed. The FDT can be applied to arrive at an approximate solution of such an ill-posed ISP under the realm of the first order Born approximation. FDT relates the Fourier transform of the measured forward scattered field with the Fourier transform of the object permittivity profile. It is assumed that the object is of finite dimension and is illuminated with a plane wave propagating in the direction of θ as shown in Figure 2(a).

Fourier diffraction theorem states that the one-dimensional (1-D) Fourier transform of the forward scattered field measured along a line gives the value of the two-dimensional (2-D) Fourier transform of the object along a semicircular arc in the spatial frequency domain [9].

Thus, when an object with a permittivity profile, $c(r)$, is illuminated with a plane wave, the Fourier transform of the forward scattered field given by $E_\theta(K_x, K_y)$ measured on the line $\eta = l$ can provide the values of the 2-D Fourier transform, $C(K_x, K_y)$, of the object's permittivity profile along a semicircular arc in the frequency domain (Figure 2(b)). Hence, if $c(r) \overset{F.T}{\longleftrightarrow} C(K_x, K_y)$, then, Fourier diffraction theorem can be used to express a mathematical relation as shown in Equation (3) [9]:

$$E_\theta(K_x, K_y) = \frac{k_0^2}{2\sqrt{k_0^2 - \alpha^2}} e^{j\sqrt{k_0^2-\alpha^2}} C\left(\alpha, \sqrt{k_0^2 - \alpha^2} - k_0\right) \tag{3}$$

where 'α' is the coordinate parameter in the frequency domain that varies between $-k_0$ and k_0.

Hence, in an imaging scenario, when the plane waves illuminate the object, the field gets perturbed due to the presence of the object. The scattered waves emanating in all directions are collected using the receiving antennas. For applying the FDT, a spatial frequency transformation of the collected scattered signals is performed using the one-dimensional Fourier transform. With the knowledge of the transformed scattered signal values, the 2D Fourier transformed version of the object contrast function, $C(K_x, K_y)$, can be computed according to the Fourier diffraction theorem using Equation (3). Finally, the 2D Fourier transform of the contrast function can be transformed back into the spatial domain to obtain the actual permittivity profile.

During practical implementation, the scattered data produced by a single illumination will not provide sufficient data for reconstruction. More views from different directions around the object are needed. Hence, a multi-illumination approach is adopted with transmitters illuminating the object from various angles around it. Each view will generate a separate semicircular arc in the frequency domain as shown in Figure 2(c). Thus, with increased number of excitations, a complete view of the object under study is made possible, which will increase the data available for reconstruction.

In this section, the initial step to solve the inverse problem has been discussed. The scattered signals are processed in accordance with the principles of the Fourier diffraction theorem which provides an approximate initial estimate of the permittivity distribution of the scatterer. This initial contrast profile is given to the deep learning module for performing the training of the network which is described in Section 2.2.

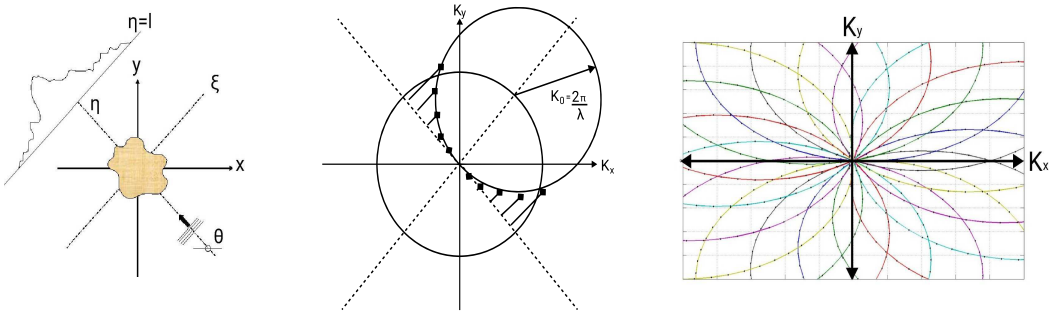

Figure 2. (a) A typical imaging setup for the acquisition of scattered data, (b) the frequency domain representation of the scattered signals along a semicircular arc for single illumination and (c) the frequency domain representation of the scattered signals along semicircular arcs for a multi-illumination scenario.

2.2. Inversion Using Deep Learning-Based Methods

In the literature of MWI, iterative methods have been the obvious choice for the inversion of full-wave nonlinear inverse scattering problems. They progressively find out the better estimates of the dielectric distribution with each iteration. However, such iterative techniques always need a finite amount of execution time ranging from several minutes to hours and are computationally exhaustive. This makes them unsuitable to perform real-time imaging. In this paper, a feasible methodology to implement

real-time imaging is proposed by making use of a state-of-the-art convolutional neural network, namely the U-net.

Traditionally, CNNs are used as classifiers i.e., the input is an image, and the network will classify this image into a particular output class/category. However, in applications such as inverse profiling, it is required for the output of the network to be an image. U-net is one such CNN which is widely used in image segmentation applications whose input and output are in the form of images. Hence, U-net is suitable to be adopted in quantitative MWI as can be inferred from recent literature [5–8]. The U-net DL network (shown in Figure 3) follows a four-layered architecture consisting of a contracting path and an expansive path shaped in the form of alphabet 'U'. The contracting path acts as a typical convolutional network, and as we move down the path the spatial information decreases while feature information increases [8]. Due to the down-sampling in contracting path, the effective receptive field of the U-net increases which can significantly improve the level of prediction accuracy at each pixel of the output image [4]. In the expansive path, the operations are performed in the reverse order to generate an output image of the required size.

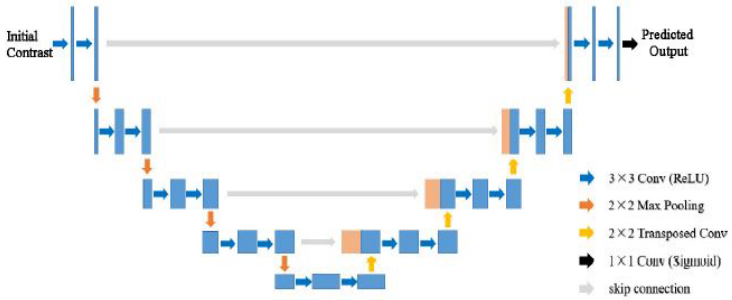

Figure 3. U-net architecture employed in the proposed method.

In this paper, a two-channel complex-valued U-net is adopted to train the real and imaginary parts of the initial contrast profile generated by applying the postulates of FDT. This is because the initial contrast profile generated is a complex profile. The U-net is a versatile network in quantitative MWI due to its potential to follow and generate a nonlinear modeling approach. This feature is imparted by the batch normalization step present in the convolutional path of the network which also makes the network more stable and accelerates the training process. Once the U-net is well trained with a large database, it becomes capable of profiling the object to be imaged accurately.

3. RESULTS AND ANALYSIS

This section presents the results using synthetic data (MNIST datasets [10], Austria profile and English alphabets) and experimental data to evaluate the performance of the proposed methodology in reconstructing the relative permittivities from the ISP. In each case, Root Mean Square Error (RMSE) has been chosen as the metric to quantitatively evaluate the performance of the algorithm. The RMSE is calculated using the following equation:

$$RMSE = \sqrt{\frac{1}{M}\sum_{m}\sum_{n}\left|\frac{\epsilon^{r}_{r;m,n} - \epsilon^{t}_{r;m,n}}{\epsilon^{t}_{r;m,n}}\right|^{2}} \tag{4}$$

where $\epsilon^{r}_{r;m,n}$ & $\epsilon^{t}_{r;m,n}$ represent the reconstructed and true dielectric permittivities of the object profile ($m = 1, 2, \ldots, M_1$; $n = 1, 2, \ldots, M_2$; $M = M_1 \times M_2$ is the total number of square cells).

3.1. Training the Network with MNIST Dataset

Initially, the network is trained and tested using the MNIST dataset [10] which is a database of 10 handwritten digits from 0 to 9. It is widely used in research works in various fields of deep learning.

The a-priori information used in inverse profiling here is that the images from the database (scatterers) are lossless and have non-negative contrast, and here, the permittivity value is set initially at 3. Each alphabet is considered to be an object to be imaged enclosed within an object domain defined by $10\lambda \times 10\lambda$, which is discretized into 32×32 grids. The background medium around the object is assumed to be air with $\epsilon_b = 1$. The object is illuminated using waves at a frequency of 3 GHz using 16 transmitter antennas. A set of 32 receiver antennas are assumed to collect the backscattered signal which are evenly distributed between 0 and 360 degrees (0 degrees included). Usually, an additive Gaussian noise is added to simulate various kinds of noise that arise in practical situations. Hence, a 30 dB Additive White Gaussian Noise (AWGN) has been added to the scattered data before inverse profiling [2, 12]. The addition is done to account for the various sources of noise that will naturally accompany any practical experiment like the faults in the measuring device, environmental errors, errors introduced by the experimenter, etc.

Initially, around 5000 images from the training dataset are subjected to the forward problem to generate the corresponding scattered signals. Thereafter, these signals are processed using the principles of FDT to generate the coarsely reconstructed version of the profile (initial contrast function). The images hence generated as the initial estimate of the dielectric distribution are now given as input to the U-net for training the network. Meanwhile, the corresponding original images from the MNIST database are set as the target towards which the network is trained. The networks are trained using the adaptive moment estimation optimizer, i.e., the ADAM optimizer with a batch size of 32, epoch setting as 100 and a learning rate of 10^{-4}. Since the U-net is trained using both the real and imaginary parts of the contrast function, the input and output of the network are all images of size $N \times N \times 2$. Out of the total 5000 images randomly chosen from the MNIST dataset, 4000 images are used in training, and the rest of the 1000 images are used for validating the established CNN within the training phase. The training of the network was performed on a small-scale server with the configuration of 32 GB access memory, Intel Xeon E5-1620v2 central processing unit, NVIDIA GeForce GTX 1050Ti. Tensor flow library was used to design and implement the U-net while the FDT algorithm was developed in the MATLAB 2021a® environment.

3.1.1. Testing the MNIST Images

Once the network has been trained, the next step is to test the efficiency of the U-net in carrying out real-time imaging. To this end, random images from the MNIST testing database are provided as input to the trained U-net. Figures 4 (a)–(c) represent the ground truth images with permittivity value of $\epsilon_r = 3$, which are given to the network for testing purposes. The corresponding reconstructed profiles produced at the output of the U-net are shown in Figures 4(d)–(f).

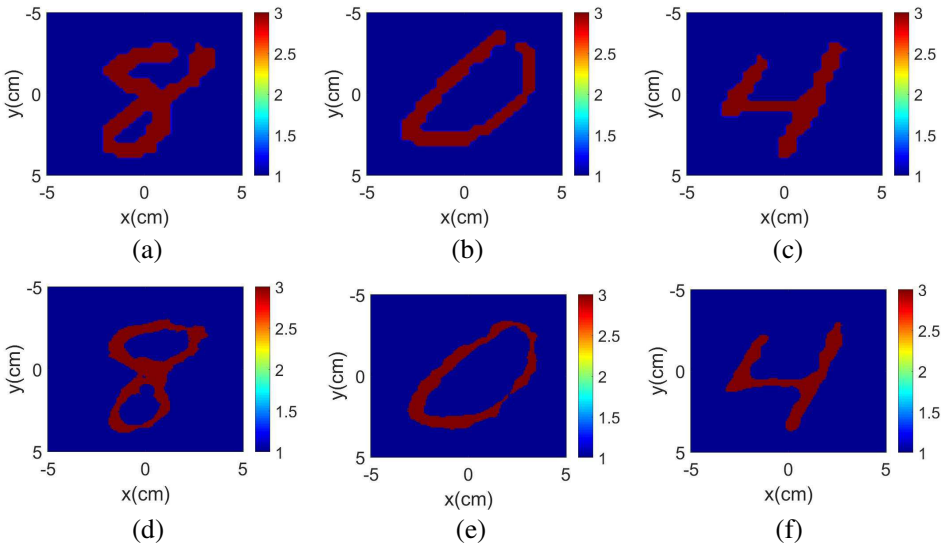

Figure 4. Reconstruction of digit-like objects with relative permittivity $\epsilon_r = 3$.

3.1.2. Testing the Combined MNIST Profile

To further test the versatility of the trained U-net, a more complex image comprising a group of 16 characters combined into a single image is considered (Figure 5(a)). The combined image reconstructed by the network is shown in Figure 5(b).

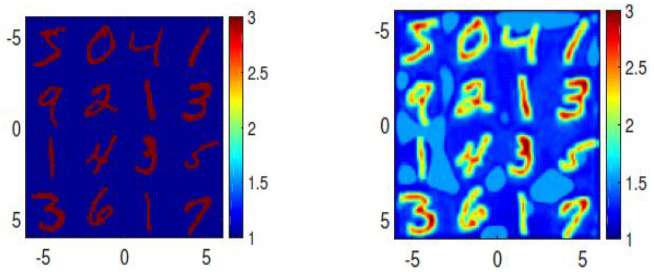

Figure 5. (a) Combined input profile and (b) the reconstructed output.

3.1.3. Testing English Alphabets

To test the trained network further, English alphabets (of permittivity 3) are given as test inputs. The network which is trained using handwritten numerical images from the MNIST database is able to reconstruct English alphabets as shown in Figure 6. The first row (Figures 6(a)–(d)) shows the ground truth images, and the imaging results obtained by the proposed method are shown in the row below (Figures 6(e)–(h)) . The conclusion drawn from this test is that in spite of training the network on images from the MNIST database satisfactory reconstruction results can still be obtained from very different objects.

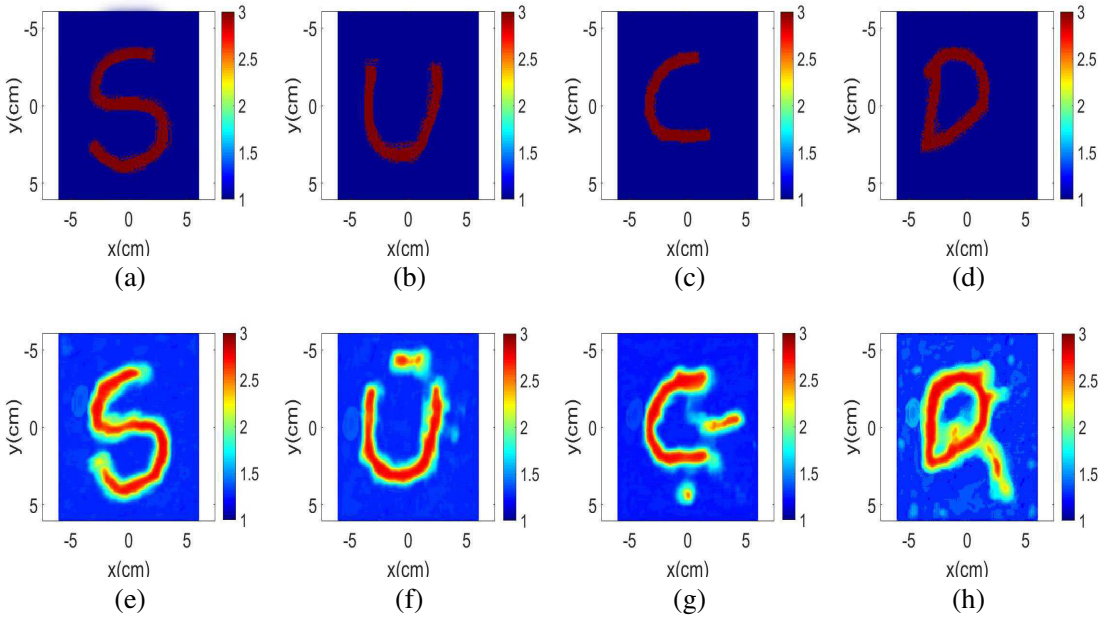

Figure 6. Reconstruction of English alphabets with relative permittivity $\epsilon_r = 3$.

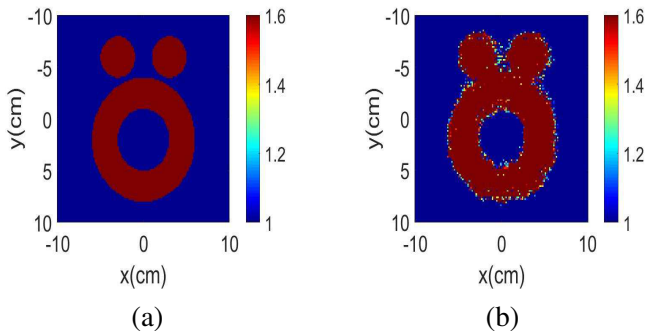

Figure 7. (a) The ground truth of the Austria Profile and (b) the reconstructed image.

3.1.4. Testing the Austria Profile

As a next yardstick, 'Austria profile' (Figure 7(a)) is chosen to validate the performance of the network under the proposed method. The Austria profile is formed of two disks and a ring. The two disks are of the same radius of 0.2 m, and their centres are at (0.3, 0.6) and (−0.3, 0.6) m, respectively. The ring present in the profile has an inner radius of 0.3 m and an outer radius of 0.6 m. The MNIST database in the permittivity range [1, 1.5] is used to train the U-net. The response of the network to Austria profile with an entirely different shape and structure is taken in order to investigate the generalization ability of the proposed learning-based method. The Austria profile is a well accepted profile in the research community engaged in various fields including the inverse scattering domain. In order to give allowance to the noise effects of a practical imaging scenario, an additive Gaussian noise of 30 dB is added before the inversion process. Figure 7(b) shows the reconstructed Austria profile using the proposed method.

To evaluate the performance of the network quantitatively, RMSE value is chosen as the metric for comparison. The RMSE value corresponding to the Austria profile reconstructed by the proposed method is computed with respect to the ground truth. Table 1 shows the RMSE value of the proposed method in comparison with three other methods, namely, the BP, BP-DSM [8], and SVBIM [2] techniques. The method described in this paper is able to attain a lower RMSE value of 0.0672. The error values depicted in the table demonstrate that enhanced results can be obtained using the proposed method over the other three methods, BP, BP-DSM, and SVBIM.

Table 1. RMSE values for the reconstructed Austria Profile for MNIST database.

Target	Reconstruction Errors
BP [8] 2020	0.1278
BP-DSM [8] 2020	0.1070
SVBIM [2] 2021	0.0813
Proposed	0.0672

3.2. Experimental Validation

The performance of the proposed method is further validated experimentally using measured data published by the Institute Fresnel, Marseille, France (named as 'FoamDielExt' database [11]). This particular experimental dataset contains scattered signal data in the frequency range of 2 GHz to 10 GHz. For the experimental setup, wide band ridged horn antennas were employed as transmitting and receiving antennas. TM illumination was considered for this setup consisting of 8 transmitters and 241 receivers. The scatterer used for the experiment is shown in Figure 8(a). It consists of two cylinders placed at a distance of 1.67 m from the antennas. The dielectric foam cylinder (blue) has relative permittivity in the range of 1.45 ± 0.15. The plastic cylinder (yellow) made of Berylon is located outside

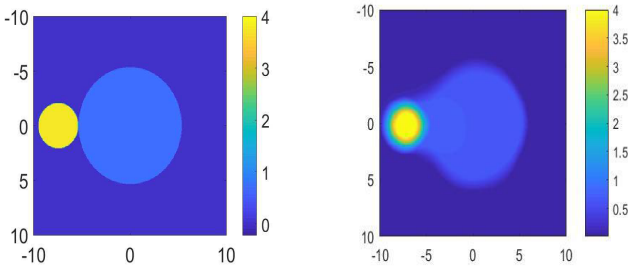

Figure 8. (a) Ground truth of the FoamDielExt database and (b) the reconstructed image.

the foam cylinder and has permittivity values between 3 ± 0.3. The radii of the two circles are 3.1 cm and 8 cm, respectively.

For the training process, a combined dataset is created by embedding a database of circular cylinders into the 5000 images taken from the MNIST dataset. Samples in the database of cylinders are synthesized in the form of cylinders with random position, size, and permittivity values. The relative permittivities of the circles were chosen in the range of $[1:3]$ such that the smaller circles have a larger randomly chosen dielectric value than the larger circles. The forward scattering is performed to generate the scattered signal values for each profile from the combined training dataset. These scattered signals are processed in accordance with the postulates of the FDT to generate the initial contrast function. Thereafter, an additive white Gaussian noise corresponding to 30 dB of input SNR is added as explained in Section 3.1. The combined dataset comprising the initial contrast profiles created from both the MNIST database and the circles database is used for training the U-net. The network is trained for 1000 epochs to minimize the RMSE between the input and the output profile.

The scattered signals available in the FoamDielExt database are now given as the testing input to the trained CNN. The network uses the method proposed in this paper to solve the inverse problem and generate a permittivity profile at its output. The reconstruction results obtained at 4 GHz are shown in Figure 8(b). For a fair comparison, the imaging domain is discretised into a mesh grid of size 32×32, and the results obtained by the proposed method are compared with the learning based hybrid method (BPDSM) [8] and SVBIM [2]. Table 2 shows the RMSE value evaluated for the proposed method and the compared methods. It can be noted that the proposed method has a maximum reduction in noise as compared with the other techniques, with an RMSE value of only 0.0922 against 0.1858, 0.1631, and 0.1037 for BP, BPDSM, and SVBIM methods.

Table 2. RMSE results for the reconstruction of profile.

Target	Reconstruction Error
BP [8] 2020	0.1858
BP-DSM [8] 2020	0.1631
Proposed method	0.0922

In this paper, FDT technique is in itself a complete non-iterative solver of the ISP. In contrast to other conventional iterative solvers that converge to the solution after multiple iterations, the FDT is a one-step solver of the ISP. Hence, the initial contrast profile generated by the FDT method is better than the profile produced by the iterative methods after only the first iteration. This is the reason for the reduced error values produced by the proposed method in comparison to [2]. Moreover, the U-net DL network used in this paper for training purpose has two channels, with each channel able to handle both real and imaginary parts of the initial contrast profile produced by applying the principles of FDT. However, in [8], only a single channel is present to handle the real valued initial contrast profile.

4. CONCLUSION

A deep learning-based approach in conjugation with Fourier diffraction theorem is proposed in this paper to solve the inverse scattering problem. The proposed methodology is adept in generating a real-time permittivity mapping of the object to be imaged. The quantitative reconstruction of the dielectric permittivity from the measured scattered field values is done in a single step as against that by a long iterative procedure employed by conventional numerical methods. The proposed technique proceeds in two stages, with the initial estimate of the contrast function being generated by the FDT in the first stage. This initial profile is fed to a trained U-net to reconstruct the final dielectric permittivities of the scatterer in the second stage. The capability of the proposed method is clearly observed from the results of numerical analysis as well as experimental validation. By comparing with similar deep learning methods like BP-DSM and SVBIM, it is found that the RMSE obtained by the proposed method is 0.0922 against 0.1631 and 0.1037.

REFERENCES

1. Benny, R., T. A. Anjit, and P. Mythili, "An overview of microwave imaging for breast tumor detection," *Progress In Electromagnetics Research B*, Vol. 87, 61–91, 2020.
2. Anjit, T. A., R. Benny, P. Cherian, and P. Mythili, "Non-iterative microwave imaging solutions for inverse problems using deep learning," *Progress In Electromagnetics Research M*, Vol. 102, 53–63, 2021.
3. Wang, F., et al., "Multi-resolution convolutional neural networks for inverse problems," *Scientific Reports*, Vol. 10, 1–11, 2020.
4. Khoshdel, V., A. Ashraf, and J. LoVetri, "Enhancement of multimodal microwave-ultrasound breast imaging using a deep-learning technique," *Sensors*, Vol. 4050, 1–14, 2019.
5. Wei, Z. and X. Chen, "Deep-learning schemes for full-wave nonlinear inverse scattering problems," *IEEE Trans. Geosci. Remote Sens.*, Vol. 57, 1849–1860, 2019.
6. Yao, H. M., W. E. I. Sha, and L. Jiang, "Two-step enhanced deep learning approach for electromagnetic inverse scattering problems," *IEEE Antennas and Wireless Propagation Letters*, Vol. 18, 2254–2258, 2019.
7. Jin, K. H., M. T. McCann, E. Froustey, and M. Unser, "Deep convolutional neural network for inverse problems in imaging," *IEEE Trans. Image Processing*, Vol. 26, 4509–4522, 2017.
8. Zhang, L., K. Xu, R. Song, X. Z. Ye, G. Wang, and X. Chen, "Learning-based quantitative microwave imaging with a hybrid input scheme," *IEEE Sensors Journal*, Vol. 20, 15007–15013, 2020, doi: 10.1109/JSEN.2020.3012177.
9. Kak, A. C. and M. Slaney, *Principles of Computerized Tomographic Imaging*, Society of Industrial and Applied Mathematics, July 2001.
10. Deng, L., "The MNIST database of handwritten digit images for machine learning research," *IEEE Signal Processing Magazine*, Vol. 29, 141–142, 2012, doi:10.1109/MSP.2012.2211477.
11. Geffrin, J.-M., P. Sabouroux, and C. Eyraoud, "Free space experimental scattering database continuation: Experimental set-up and measurement precision," *Inverse Probl.*, Vol. 21, 117–130, 2005.
12. Li, L., et al., 'DeepNIS: Deep neural network for nonlinear electromagnetic inverse scattering," *IEEE Trans. Antennas and Propag.*, Vol. 67, 1819–1825, 2019.